Electric Vehicle Charging Facility as a Smart Energy Microhub

Walied Alharbi, *Student Member, IEEE*, and Kankar Bhattacharya, *Senior Member, IEEE*

***Abstract*—This paper presents a novel framework for designing an electric vehicle charging facility (EVCF) as a smart energy microhub from the perspectives of both an investor and a local distribution company. The proposed framework includes a Vehicle Decision Tree, a Queuing Model, a Distribution Margin Assessment Model, a Distributed Generation (DG) Penetration Assessment Model, an Economic Assessment Model, and a Distribution Operations Model. Three design options for the EVCF are examined, battery energy storage systems (BESS), renewables based DG, and a microhub that incorporates both BESS and renewables based DG with the option of exchanging power with the main grid. Test results considering a 33 bus distribution system and realistic vehicle statistics extracted from the 2009 (US) National Household Travel Survey are presented and discussed. The findings demonstrate the effectiveness of the proposed smart energy microhub design framework.**

***Index Terms*— Battery energy storage system, Electric vehicle charging facility, Microhub, Queuing theory.**

I. Nomenclature

Sets and Indices

i, j	Index for buses, $i, j \in$N.
k	Index for time periods, $k \in K$.
l	EVCF buses, $l \in N$.
s	Index for season, $s \in$ summer, winter.
SS	Subset for substation buses, $SS \in N$.
y	Set of years in plan horizon, $y \in Y$.

Parameters

μ	Charging service rate.
c	Number of fast chargers of EVCF.
C^{TH}	Transformer capacity for EVCF.
$\underline{EPR}, \overline{EPR}$	Minimum and maximum energy to power ratio for a given BESS type.
$E[Z]$	Expected number of occupied fast chargers.
IC^E	Variable installation cost associated with BESS energy size [$/kWh].
IC^P	Variable installation cost associated with BESS power size [$/kW].
IC^{PV}	PV generation installation cost [$/kW].
M^C	Fast charger maintenance cost [$/KVA].
M^{TH}	Transformer maintenance cost [$/kVA].
n	Number of discharged PEVs at an EVCF.
Nd	Number of days in a season.
OM^f	Annual fixed operation and maintenance (O&M) cost of BESS [$/kW].
OM^{PV}	Fixed O&M cost of PV energy [$/kWh].
OM^V	Variable O&M cost of BESS [$/kWh].
P_{AVG}	Average power per fast charger [kW].
PD, QD	Active and reactive power demand [p.u].
$P^{DG\text{-}Max}$	Maximum penetration of connected DG [p.u].
PD^{PEV}	Expected demand of an EVCF [kW].
PPV	Available photovoltaic output power as a percentage of its rated capacity [%].
α	Discount rate [%].
η^C	Efficiency of a fast charger [%].
η^{IN}, η^{OUT}	BESS Charging/discharging efficiency [%].
η^{PV}	PV array inverter conversion efficiency [%].
λ	Probability of PEV arrival at an EVCF.
ρ	Contract price of energy exported to grid by EVCF [$/kWh].
ρ^{MG}	Main grid electricity price [$/kWh].
ρ^{PEV}	Price for charging PEV [$/kWh].
ψ	Probability of occupied fast chargers.

Variables

C^E	Cumulative BESS energy capacity [kWh].
C^{PV}	Cumulative solar PV capacity [kW].
E^{EX}	Energy exported to the main grid [kWh].
E^{SH}	PEV energy shedding at an EVCF [kWh].
NC^E	New BESS energy capacity [kWh].
NC^P	New BESS power capacity [kW].
NC^{PV}	New PV power capacity [kW].
P, Q	Active and reactive substation power [p.u].
P^{EX}	Power exported to the main grid [kW].
P^{IM}	Power imported from the main grid [kW].
P^{IN}, p^{OUT}	BESS charging/discharging power [kW].
P^{SH}	PEV load shedding at an EVCF [kW].
$Psize^{BESS}$	Cumulative BESS power capacity [kW].
P^{UN}	Unserved power in distribution system [p.u].
RC	Annual cost of new EVCF design [$].
RC^{Inv}	Investment cost of a new design [$].
RC^{OM}	O&M cost of an EVCF [$].
SOC	BESS state of charge [kWh].
U^{EX}, U^{IM}	Exporting/importing binary variable: 1 when power is exported/imported to/from the main grid and 0 otherwise.
V	Voltage magnitude [p.u].

W. Alharbi and K. Bhattacharya are with the Department of Electrical and Computer Engineering, University of Waterloo, Waterloo, ON, N2L3G1, Canada (email: walharbi@uwaterloo.ca; kankar@uwaterloo.ca).

The first author wishes to acknowledge the financial support received from Majmaah University, Saudi Arabia, through the Saudi Cultural Bureau, Ottawa, Canada, to carry out this research.

β	DG capacity of an EVCF site [p.u].
γ	Load serving capability [p.u].
δ	Voltage phase angle [p.u].

II. Introduction

IN light of the growing concerns of global warming and depletion of petroleum resources, plug-in electric vehicles (PEVs) have been receiving significant attention in recent years [1]-[2]. It is recognized that comprehensively designed Electric Vehicle Charging Facilities (EVCFs) are vital for facilitating PEV penetration and their public acceptance. Investigating the feasibility of future accommodation of multiple EVCFs in power grids is important. Because fast charging occurs most frequently during evening hours, often coinciding with the peak demand, a distribution system planner must know how much load is expected to be served, as penetration of PEVs are expected to increase over the coming years.

EVCFs can also serve as sources of capacity support for the distribution system when they are equipped with battery energy storage systems (BESSs) and/or photovoltaic (PV) generation. An EVCF can provide such capacity support through appropriate considerations at the design stage by proper sizing of BESS and PV units. However, a more efficient way would be to control the PEV charging demand and offer a capacity support service to the distribution system during critical conditions. Such a design of an EVCF renders it a *smart energy microhub*, providing capacity support to the distribution system, reducing losses, and deferring upgrades. Such design may also contribute to decreased EVCF operating costs because of PV generation and energy from BESS.

The focus of this research is to explore the possibility of EVCFs operating as smart energy microhubs, with various in-built energy resources (possibly renewables based) within its facility with the provision for bi-directional energy exchange with the external grid. The energy hub can be recognized as a generalization or extension of a network node in an electric power system that exchanges power with the surrounding systems, primary energy sources, loads, and other components via multi-energy input and output ports [3]. A simple architecture of the EVCF as a *smart energy microhub* is presented in Fig. 1. The smart energy manager, which is the central controller, is the main control interface between the upstream grid and the EVCF energy resources. It has the responsibility of optimizing the operation of the *smart energy mcirohub*.

The following research questions often arise with respect to EVCF design: Would such design be economically viable for an investor while also being technically acceptable for the local distribution company (LDC)? Furthermore, when multiple EVCF locations are under consideration, to what extent can the distribution system accommodate the EVCFs? What EVCF design is most appropriate at a specific location in order to provide mutual benefits to both the investor and the LDC? What power and energy size of a BESS and/or PV generation are needed at an EVCF location? The primary focus of this paper is to address these research questions.

A number of papers have discussed the design, planning, and operational analysis of an EVCF in distribution systems [4]-[10]. To optimize the siting of EVCFs in a distribution system, a two-stage screening method that takes into account environmental factors and EVCF service radius is proposed in [4]; then an optimal EVCF sizing model is developed for the short-term, *i.e.,* 3-year horizon. For the planning of an integrated power distribution system and EVCF, a multi-objective collaborative planning model is proposed in [5], with minimization of the overall annual investment costs and energy losses, and maximization of the annual captured traffic flow. Brenna et al. [6] examine the benefits of using PV systems as the energy supplier for charging PEVs. A mathematical model that considers the power flow related to PV generation, the EVCF, and the power grid is developed as a means of representing an urban-scale integrated system. Machiels et al. [7] studied the technical design criteria for an EVCF, including mobility needs. The findings indicated that 99.7% of the PEVs visiting an EVCF can begin charging within 10 min, based on a configuration of five charging poles; otherwise, additional charging poles are required to accommodate PEV drivers who are unwilling to wait.

A solar parking lot for efficiently operating a slow EVCF is reported in [8]. The facility is a grid-tied parking lot that charges PEVs via an overhead PV array, and exports the excess power to the main grid. When power shortages occur, power is imported from the grid. The design of an EVCF with a BESS as a solution for low-voltage feeders with high PV penetration is discussed in [9]; a mixed integer linear programming model is proposed for determining the BESS charging schedule for voltage regulation. Liu et al. [10] studied the function and effect of small-sized superconducting magnetic energy storage system in an EVCF that included PV generation. An energy management strategy that focused on voltage stability of the dc bus and the energy transfer among the resources is developed.

From the brief review of literature, it is noted that most of the work concentrated on the technical aspects of EVCF design without taking into account the economic viability of such an investment. Furthermore, there is a need to examine how the EVCF functionalities can be adopted to the smart grid environment considering BESS and other renewables based DG options in this design, from the perspectives of the investor and the LDC. Also, none of the reported works examined how the charging load profile will impact the EVCF configuration considering realistic penetration of PEVs in the long term. To this effect, three new design options are considered in this paper, Design-1: EVCF with BESS, Design-2: EVCF with renewables based DG, and Design-3: EVCF as a *smart energy microhub*.

The main contributions of the work presented in this paper are as follows:

1) A novel framework is proposed for the optimal design and sizing of an EVCF as a *smart energy microhub* that optimally controls the energy flow between the PV unit, the BESS, the external grid, and local consumption.

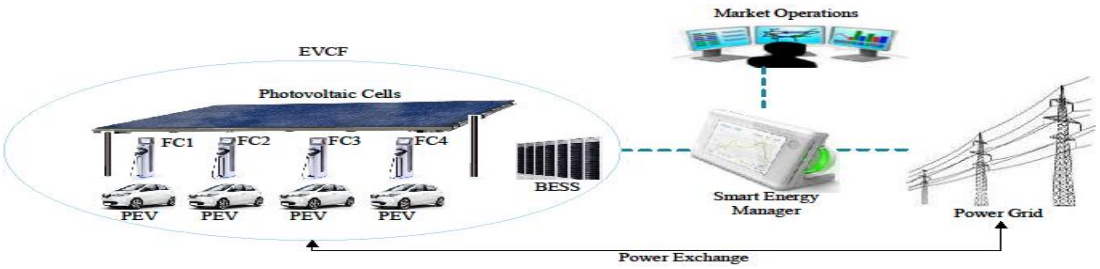

Fig. 1 A simple architecture of the EVCF as a *smart energy microhub*

2) The proposed framework is based on a 'bottom-up approach' to the design and planning of an EVCF, incorporating a detailed representation of vehicle mobility statistics in order to estimate the charging load profile, and then integrating all dimensions of planning, such as technical feasibility assessment, economics, and distribution system operations impact assessment.
3) The proposed framework represents a new business model for an EVCF investor that, in addition to profit, considers the economic benefits to the EVCF from exchanging power with the external grid, while also taking into account the advantages of such integration for the LDC.
4) The presented work facilitates and encourages the penetration of sustainable energy resources through the creation of smart energy hubs within a distribution system, which helps reduce greenhouse gas emissions.
5) The implementation of this framework is envisaged to help defer, or even avoid, investments in grid reinforcement over the long-term, based on the provision of capacity support for the distribution system and a reduction of the impact of rapid PEV charging loads on the grid.

In view of the above, the primary objectives of the work presented in this paper are as follows:

1) Propose a Vehicle Decision Tree (VDT) using realistic vehicle statistics extracted from the 2009 (US) National Highway Travel Survey (NHTS) data [11] to predict times PEVs need fast charging in rural and urban areas, and develop a Queuing Model (QM) to estimate the charging load for multiple PEVs served at a rapid EVCF, considering medium and high PEV penetration levels in the long-term.
2) Examine the effects of PEV penetration levels on the PEV charging demand profile and hence arrive at an appropriate configuration of the rapid EVCF, such as the required number of fast chargers, and the transformer capacity.
3) Propose a novel framework for designing the EVCF as a *smart energy microhub* and hence determine the optimal investment decisions and appropriate design options at a specific location in the distribution system, from both the investor's and the LDC's point of view.
4) Assess distribution system capability to accommodate multiple EVCFs in the long-term, with and without the new design of EVCFs.

The paper is structured as follows. The proposed framework is introduced and its mathematical models are explained in detail in Section III. The test system considered, and the assumptions underlying the validation of the framework are presented in Section IV. Section V presents analysis and discussion of the findings to demonstrate the effectiveness of the proposed framework. Section VI outlines the conclusions drawn based on the numerical results.

III. Proposed Framework

The proposed framework includes a VDT, QM, a Distribution Margin Assessment Model, a DG Penetration Assessment Model, an Economic Assessment Model (EAM), and a Distribution Operations Model. Fig. 2 shows the architecture of the proposed framework, the linkages between the models, the input parameters, and the output decisions associated with them. The probability of PEV arrival per hour (λ) at an EVCF is modeled based on a VDT that uses realistic vehicle statistics extracted from [11]. The QM expresses the overall charging process for multiple PEVs served at the EVCF and estimates the expected PEV charging demand. The Distribution Margin and DG Penetration Assessment Models determine the maximum load serving capability and the maximum DG capacity that can be accommodated, respectively, at an EVCF bus over the planning period. The EAM facilitates a prospective investor to arrive at an optimal plan with respect to investment in new design of an EVCF. The Distribution Operations Model evaluates the effectiveness of the new EVCF design for distribution system operations and determines the desirable design options from the LDC's perspective. The five mathematical models are discussed in detail in the following subsections.

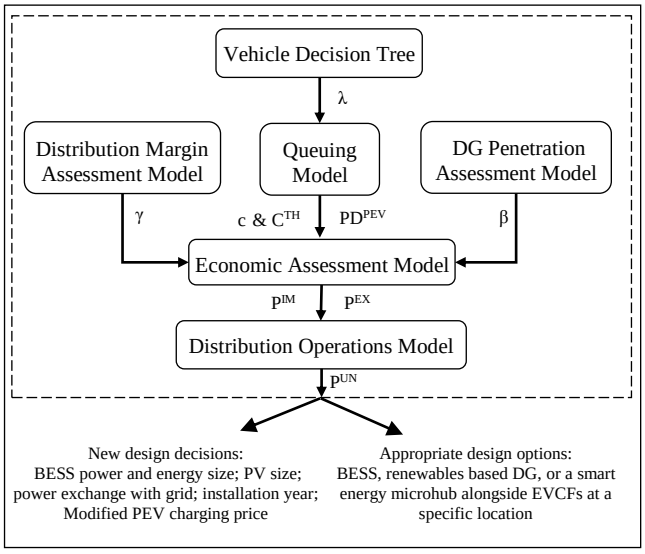

Fig. 2 Architecture of the proposed framework for design decisions of an EVCF as a *smart energy microhub*.

A. Vehicle Decision Tree (VDT) and Queuing Model (QM)

To estimate the probabilistic arrival rate of PEVs per hour, detailed transportation data is needed. The distribution of trip distances, the time-of-day distribution of the trips, and the number of trips associated with each vehicle are extracted from [11] and are used for predicting the required times for PEV fast charging. Because of the lack of data pertaining to the travel patterns of PEVs, these are assumed to be similar to those of traditional vehicles, thus enabling the use of the same NHTS data set. The λ parameter is modeled using the proposed VDT, as presented in Fig. 3. For each trip, the battery state of charge (SOC) of a PEV is checked considering its distance-driven mileage, and when the PEV depletes the entire SOC window, either the start time or the end time of that trip is recorded. The following set of rules are used:

a) A PEV, fully-charged at the start of a trip, will completely deplete its charge if the trip mileage is greater than the mileage driven on electricity. Such vehicles are excluded from the VDT model, since their battery types are not appropriate for such trips.
b) If the trip mileages are smaller than the mileage driven on electricity, the PEV will complete one or more trips, but will deplete its charge in the middle of a trip. For such cases, the start time of that trip will be recorded for a fast charge, which helps avoid trip interruptions.
c) If the trip is completed prior to depletion of charge, the finish time of that trip is recorded, to avoid trip interruptions.
d) To reduce the computational time, any vehicle whose cumulative mileage for daily trips is less than 20 miles is excluded, since such vehicle will not need fast charging.

However, since no geospatial data was available for correlating the distance of the vehicles from a central charging facility, the outcome of the VDT is presented as the probability of a vehicle call for charging, rather than that of a vehicle arrival at the EVCF. To compensate for the missing information on distances between the PEVs and the EVCF, the following points have been taken into consideration:

1) Point-a: The exact time between a PEV call for a fast charge and the arrival of that PEV at an EVCF is unknown and is dependent only on the distance from the *point of call* to the EVCF. The *point of call* is the location of the PEV when the minimum SOC signal is activated in the vehicle, it is similar to the low fuel indicator of traditional cars. From this *point of call*, the PEV driver is expected to drive directly to an EVCF. Each PEV will have its own *point of call* and consequently the associated driving distances from that *point of call* to the EVCF is an uncertain parameter. The hour, rather than the minute, when the PEV calls for a fast charge is therefore considered for estimating the probability of PEV arrival at an EVCF each hour, based on the assumption that the PEV will definitely reach the local EVCF within that one-hour calling window. Indeed, using arrival rates on a per hour basis allows a wider range of time for the PEV to arrive at an EVCF.

   In order to record the hour rather than the minutes when the PEV calls for a fast charge, the minutes are rounded to the nearest hour, except for exact half-hour calls, which are rounded down (*for example, call at 15:30 is rounded to 15:00*).
2) Point-b: US gasoline fueling facilities numbered nearly 160,000 in 2010 [12], or about one facility for every 1500 vehicles. Assuming a similar use of one or two fills per week, one EVCF is chosen for addressing the needs of a few hundred PEVs. In this work, each EVCF is considered to be serving up to 20% of the total forecasted number of vehicles in the distribution system, which represents the transformation percentage for a few hundred PEVs, for each year of the planning period.

In such a design-planning problem, from the EVCF investor's perspective, in order to estimate the expected demand, two important pieces of information must be known: when the charging demand is expected to take place, and how much power is required. The VDT for the first consideration (Point-a) estimates when the charging demand will take place for each hour, while the VDT for the first and second considerations (Point a and b) determines how many PEV arrivals will occur per hour. The results are then incorporated into the QM for use in the estimation of the PEV charging demand.

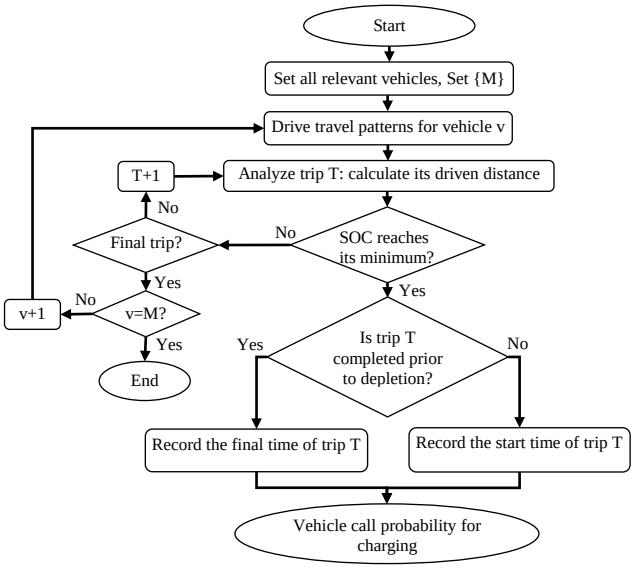

Fig. 3 Flow chart of the proposed Vehicle Decision Tree

Queuing theory [13]-[15] is employed to describe the overall process of charging multiple PEVs served at a rapid EVCF. Using the VDT and *M/M/c* queuing theory [13], the expected PEV charging demand is estimated. PEVs at an EVCF can be considered queuing customers that may have to wait at the EVCF in order to charge their batteries.

In line with reported research [14], [15], the following conditions are assumed at the EVCF:

1) PEV inter-arrival times are independent and exponentially distributed because the arrival of one PEV carries no information about the arrival of another, hence making it a Poisson process.

2) For the same reason, the hourly service rates for charging PEVs at an EVCF are independent and exponentially distributed, and are also categorized as Poisson process.
3) The EVCF has *c* identical fast chargers.
4) A first-come-first-served rule is applied for charging PEVs, which form a single queue upon arrival.
5) The EVCF has a large enough waiting space for PEVs, which means, that no vehicle is rejected from entering the queuing system. Hence the M/M/c/k queuing model, where *k* refers to 'limited capacity' of the EVCF can be effectively represented as an M/M/c/∞ queuing model. This assumption is validated through a case study in a later section of the paper.

These assumptions allow the charging service at an EVCF to be modelled as an *M/M/c* queuing model. Based on this QM formulation [13], the system is stable if and only if the occupation rate of the fast chargers is less than unity, the occupation rate denotes the probability that a fast charger is occupied. It can be determined for each hour by dividing the probabilistic arrival rate of PEVs at the EVCF by the number of identical fast chargers at the EVCF and by the charging service rate, and can be expressed as follows:

$$\psi(k) = \frac{\lambda(k)}{c\mu(k)} \leq 1 \tag{1}$$

Based on (1) and a sufficient condition for the stability of the QM, the minimum number of fast chargers that ensures a stable EVCF queuing system [13] should adhere to the following inequality:

$$c > \frac{\lambda(k)}{\mu(k)} \quad \forall k \tag{2}$$

The determination of the expected number of occupied fast chargers is based on a limiting-state probability that *n* discharged PEVs are present at the EVCF [13]:

$$P_n(k) = \begin{cases} \frac{1}{n!}\left(\frac{\lambda(k)}{\mu(k)}\right)^n P_0 & if\ 0 \leq n \leq c-1 \\ \frac{1}{c!c^{n-c}}\left(\frac{\lambda(k)}{\mu(k)}\right)^n P_0 & if\ n \geq c \end{cases} \tag{3}$$

where P_0 is defined as follows:

$$P_0 = \left[\sum_{n=0}^{c-1} \frac{1}{n!}\left(\frac{\lambda(k)}{\mu(k)}\right)^n + \frac{1}{c!}\left(\frac{\lambda(k)}{\mu(k)}\right)^c \left(\frac{c\mu(k)}{c\mu(k)-\lambda(k)}\right)\right]^{-1} \tag{4}$$

If *n* discharged PEVs are present at the EVCF, the number of occupied fast chargers is given by min(*n*, *c*). Based on [13], the expected number of occupied fast chargers *E[Z]* can hence be calculated as follows:

$$E[Z(k)] = \sum_{n=0}^{\infty} P_n(k) \min(n,c) = \frac{\lambda(k)}{\mu(k)} \tag{5}$$

The last step is to estimate the power demand (PD^{PEV}) of the EVCF by multiplying the average power per fast charger by the expected number of occupied fast chargers, as follows:

$$PD^{PEV}(k) = E[Z(k)] \cdot P_{AVG} \tag{6}$$

B. Distribution Margin Assessment Model

Objective Function: Maximize the load serving capability at an EVCF bus in the distribution system, as follows:

$$J_1 = \sum_{l \in N} \sum_{k \in K} \sum_{s \in S} \sum_{y \in Y} \gamma_{l,k,s,y} \tag{7}$$

The following constraints apply:

Power Flow Equations: The power injected at the substation net of the load is governed by traditional power flow equations, as follows:

$$P_{i,k,s,y} - PD_{i,k,s,y} - \gamma_{l,k,s,y} = f\left(V_{i,k,s,y},\ \delta_{i,k,s,y}\right) \quad i \forall N, \forall k, \forall s, \forall y \tag{8}$$

$$Q_{i,k,s,y} - QD_{i,k,s,y} = f\left(V_{i,k,s,y},\ \delta_{i,k,s,y}\right) \quad i \forall N, \forall k, \forall s, \forall y \tag{9}$$

Additional grid operational constraints, such as substation capacity limits, bus voltages and feeder power flow limits are also imposed.

C. DG Penetration Assessment Model

This model estimates the maximum DG capacity that can be accommodated at an EVCF bus, over the planning period. The objective function is given as follows:

$$J_2 = \sum_{l \in N} \sum_{k \in K} \sum_{s \in S} \sum_{y \in Y} \beta_{l,k,s,y} \tag{10}$$

Real Power Flow Equation:

$$P_{i,k,s,y} - PD_{i,k,s,y} + \beta_{l,k,s,y} = f\left(V_{i,k,s,y},\ \delta_{i,k,s,y}\right) \quad i \forall N, \forall k, \forall s, \forall y \tag{11}$$

Maximum Reverse Power Flow Constraint: This constraint ensures that the allowable DG penetration that causes the maximum reverse power flow for the minimum load condition is limited. In this study, the minimum load condition occurs at *y =0*. According to technical specifications applicable in

Ontario, Canada [16], the maximum reverse active power flow is limited to 60% of the main substation rating. Accordingly,

$$\sum_{l\in N}\beta_{l,k,s,y} \le \sum_{i\in N} PD^{Min}_{i,k,s,0} + 0.6S^{Cap}_{ss} \quad (12)$$

Maximum Bus Connection Constraint: Based on the voltage level and the technical constraints associated with the LDC, the maximum capacity of the DG connection at any bus is limited, as follows:

$$\beta_{l,k,s,y} \le P_l^{DG-Max} \qquad \forall l \quad (13)$$

In addition to the above, (9) and grid operational limits are also included in this model.

D. Economic Assessment Model (EAM)

Objective Function: Maximize the net present value of an investor's profit over the useful life of the new design of the EVCF.

$$J_3 = \sum_{y=0}^{Y} \frac{(REVy - RCy)}{(1+\alpha)^y} \quad (14)$$

where *REVy* denotes the total EVCF revenue in year *y*, which includes the revenue accrued from charging PEVs and selling any available energy to the main grid, as given by:

$$REV_y = \left(\left[\sum_{k=1}^{24}\sum_{s=1}^{2} \rho^{PEV}_{k,s}\cdot PD^{PEV}_{k,s}\right]Nd_s\right)_y + \rho E^{Ex}_y \quad (15)$$

In (16), the total annual cost of new investment and various O&M cost components of the EVCF are as follows:

$$RC_y = RC^{Inv}_y + RC^{OM}_y \quad (16)$$

where

$$RC^{Inv}_y = IC^E NC^E_y + IC^P NC^P_y + IC^{PV} NC^{PV}_y \quad (17)$$

$$RC^{OM}_y = OM^f Psize^{BESS}_y + M^{TH} + M^C + OM^{PV} C^{PV}_y + \left(\left[\sum_{k=1}^{24}\sum_{s=1}^{2}\rho^{MG}_{k,s}\cdot P^{IM}_{k,s} + OM^V \eta^{OUT} P^{OUT}_{k,s}\right]Nd_s\right)_y + (\rho + 0.5)E^{SH}_y \quad (18)$$

The first and second terms of (17) represent the installation cost of the BESS, while the third term is the installation cost of PV generation. Equation (18) denotes the EVCF operating and maintenance costs, including that of the BESS, the transformer and fast charger, and PV generation operating and maintenance costs, the operation cost of importing power from the main grid, and the cost of shedding PEV charging loads which may occur when the PV generation (Design-2) is only considered. The cost of PEV energy shedding is considered to be higher than the energy export price, in order to limit this action for solution feasibility only. The energy shedding is defined as:

$$E^{SH}_y = \left(\left[\sum_{K=1}^{24}\sum_{s=1}^{2} P^{SH}_{k,s}\right]Nd_s\right) \qquad \forall y \quad (19)$$

The following constraints apply:

Demand Supply Balance of EVCF: Total generation meets the demand at period *k* on winter and summer days in year *y* at an EVCF.

$$P^{PV}_{k,s,y} + P^{IM}_{k,s,y} + P^{OUT}_{k,y} + P^{SH}_{k,s,y} = PD^{PEV}_{k,s,y} + P^{EX}_{k,s,y} + P^{IN}_{k,s,y} \qquad \forall k, \forall s, \forall y \quad (20)$$

Where $P^{PV}_{k,s,y} = C^{PV}_y PPV_{k,s}$

Distribution Grid Interaction Limits: These constraints are included so as to avoid oversizing or undersizing the BESS and/or PV generation capacity for the EVCF.

$$0 \le P^{IM}_{k,s,y} \le \gamma_{k,s,y} U^{IM}_{k,s,y} \qquad \forall k, \forall s, \forall y \quad (21)$$

$$0 \le P^{EX}_{k,s,y} \le \beta_{k,s,y} U^{EX}_{k,s,y} \qquad \forall k, \forall s, \forall y \quad (22)$$

$$U^{IM}_{k,s,y} + U^{EX}_{k,s,y} \le 1 \qquad \forall k, \forall s, \forall y \quad (23)$$

Energy Export Limits: These limits ensure that the energy exported is only from the solar PV generation and does not include the BESS energy. Since there is no incentive price yet for installing a BESS in Ontario, these constraints ensure that the contract price of Ontario PV generation cannot be used for exporting power to the main grid from the BESS. Moreover, it would be unprofitable to use the Hourly Ontario Electricity Price (HOEP) for exporting power to the main grid from the BESS, as compared to its high installation costs. Thus, the BESS is solely used for managing the EVCF energy consumption and not for selling energy to the main grid.

$$E^{EX}_y \le \eta^{PV}\left(\left[\sum_{K=1}^{24}\sum_{s=1}^{2} C^{PV}_y PPV_{k,s}\right]Nd_s\right) \qquad \forall y \quad (24)$$

$$E^{EX}_y = \eta^{PV}\left(\left[\sum_{K=1}^{24}\sum_{s=1}^{2} P^{EX}_{k,s}\right]Nd_s\right) \qquad \forall y \quad (25)$$

BESS Balance Constraint: This constraint is formulated using a simplified book-keeping model for the SOC of the BESS as follows [17]:

$$SOC_{k+1,s,y} = SOC_{k,s,y} + \left(P^{IN}_{k,s,y}\eta^{IN} - P^{OUT}_{k,s,y}/\eta^{OUT}\right).\Delta t \quad \forall k, \forall s, \forall y \quad (26)$$

$$0.2C_y^E \le SOC_{k,s,y} \le C_y^E \qquad \forall k, \forall s, \forall y \tag{27}$$

where Δt is considered to be one hour for this study.

BESS Power Limits and Initial/Final Status of the SOC: The power drawn or discharged by the BESS is constrained by the limits, as follows:

$$P_{k,s,y}^{IN} \le Psize_y^{BESS}, P_{k,s,y}^{OUT} \le Psize_y^{BESS} \qquad \forall k, \forall s, \forall y \tag{28}$$

The initial and final status of the SOC are assumed to be 50% of BESS energy capacity. Hence,

$$SOC_{k,s,y} = 0.5C_y^E, \quad k = 1 \& k = 24, \forall s, \forall y \tag{29}$$

BESS Energy-to-Power Ratio and Maximum Discharge Time: Each battery technology has a specific range of energy-to-power ratios and maximum discharge times. The range of the energy size for a specific power size is thus constrained as follows:

$$\underline{EPR} \cdot Psize_y^{BESS} \le C_y^E \le \overline{EPR} \cdot Psize_y^{BESS} \qquad \forall y \tag{30}$$

This constraint also determines the maximum discharge time at the rated power.

Dynamic Constraint on Solar PV and BESS Capacity Additions: These limits ensure that the solar PV capacity, and the power and energy capacity of the BESS for the next year are the cumulative sum of the new capacity installed plus the existing capacity.

$$C_{y+1}^{PV} = C_y^{PV} + NC_y^{PV} \qquad \forall y = 1,2,..., (T-1) \tag{31}$$

$$C_y^{PV} = NC_y^{PV} \qquad y = 1 \tag{32}$$

$$C_{y+1}^{E} = C_y^{E} + NC_y^{E} \qquad \forall y = 1,2,.., (T-1) \tag{33}$$

$$C_y^{E} = NC_y^{E} \qquad y = 1 \tag{34}$$

$$Psize_{y+1}^{BESS} = Psize_y^{BESS} + NC_y^{P} \qquad \forall y = 1,2,.., (T-1) \tag{35}$$

$$Psize_y^{BESS} = NC_y^{P} \qquad y = 1 \tag{36}$$

Constraint on Terminal Year Investment: The solar PV capacity and the BESS power and energy capacity remain unchanged beyond the planning period, implying that no new investment takes place beyond year *T*; thus,

$$C_{y+1}^{PV} = C_y^{PV} \qquad \forall y = T \tag{37}$$

$$C_{y+1}^{E} = C_y^{E} \qquad \forall y = T \tag{38}$$

$$Psize_{y+1}^{BESS} = Psize_y^{BESS} \qquad \forall y = T \tag{39}$$

E. Distribution Operations Model

Once the EVCF design is acceptable from an investor's perspective, this model is used to evaluate the investment decisions and determine the most desirable design for that specific site from the LDC's point of view.

Objective Function: Minimize the unserved power in the distribution system, as follows:

$$J_4 = \sum_{i \in N} \sum_{k \in K} \sum_{s \in S} \sum_{y \in Y} P_{i,k,s,y}^{UN} \tag{40}$$

Subject to the following constraint:

Power Flow Equation:

$$P_{ss,k,s,y} - PD_{i,k,s,y} - P_{l,k,s,y}^{IM} + P_{l,k,s,y}^{EX} + P_{i,k,s,y}^{UN} = f\left(V_{i,k,s,y}, \ \delta_{i,k,s,y}\right) \qquad i \forall N, \forall k, \forall s, \forall y \tag{41}$$

The power imported and exported by the EVCF in (41) are determined from the EAM. In addition to the above, this model also includes (9) and grid operational constraints. In the above proposed framework, the models- Distribution Marian Assessment Model, DG Penetration Assessment Model, and Distribution Operation Model are nonlinear programming problems, solved using the MINOS solver in General Algebraic Modeling System environment, while the EAM is a mixed integer nonlinear programming problem solved using the DICOPT solver [18].

IV. Test System and Simulation Data

The 33-bus radial distribution system described in [19] is employed in this study. The system peak demand is 3.8 MW in year-0, with a base voltage of 12.66 kV. All loads are assumed to be residential and grow 3% annually. Profiles of the system loads are from the IEEE Reliability Test System [20]. Winter and summer seasons are both considered, each season is represented by 24 weekday hours. It should be mentioned that the location of the EVCF is determined from a detailed planning analysis that includes technical, environmental, and economic studies, the results of which are assumed as input and are beyond the scope of this paper. Otherwise spatial components of PEV trips cannot be ignored. Furthermore, the EVCF locations would affect PEV charging behavior, and therefore there should be a feedback to the VDT. The VDT should ideally incorporate EVCF locations as one of the features. However, this work does not consider optimal siting of EVCFs, and EVCF locations are considered to be decided, for example, at Buses 15, 22, 25, and 31. Therefore, in our work, it can be assumed that the VDT has already incorporated the EVCF location aspects, and their impacts on charging behavior to arrive at the charging load profile.

The maximum penetration of connected DG at each bus is 10 MW [16]. The maintenance cost of transformers and fast chargers are 11.96 \$/kVA-year and 8.92 \$/kVA-year, respectively [4]. The charging price is assumed to be 0.06 \$/kWh. Three years of historical data from May 2012 to May 2015 [21] are used to generate the average HOEP for typical

winter and summer days, which is considered to be the main grid price (ρ^{MG}) in this paper. Each EVCF is assumed to serve up to 20% of the total forecasted number of PEVs in the distribution system, on a typical day. Four EVCFs thus serve 80% of the total number of PEVs forecasted to be in the system, and the remaining 20% are assumed to be charged somewhere else, for example, by Level-2 charging at workplace/commercial buildings. This assumption is viewed as reasonable, given the fact that fast charging is still not dominant, and it would thus be unrealistic to assume that such charging would supply the needs of all PEVs in the distribution system. Medium and high PEV penetration levels over the period 2020 to 2030 are considered [22]. Based on an average monthly residential electricity consumption of 1500 kWh, the average hourly residential load is calculated to be 2.08 kW. The total number of houses in the distribution system in year-0 is calculated to be 1486, and is assumed to grow at 1.08% annually [23]. According to the NHTS data, the average number of vehicles per household is estimated to be 1.9. Based on the knowledge of PEV penetration level, number of houses, and average number of vehicles per household, the number of PEVs in the system can be determined for each year of the planning period.

Historical hourly temperature and insolation data from Solar Radiation Research Laboratory for the period from May 2012 to May 2015 is used along with the empirical model described in [24] to estimate PV array dc output power for typical winter and summer days. The PV output power, as a percentage of its rated capacity, is determined by dividing the PV array dc output power by its rated power. The average forecast installed costs of PV generation, within planning periods is given in [25]. The fixed O&M cost of PV generation is 19 $/kW-year. The 2012 revised contract price of 0.549 $/kWh applicable in Ontario for PV generation facilities (ρ) is considered in this paper [26]. The inverter conversion efficiency of the PV array is assumed to be 95%.

Due to its low self-charge level, low energy-specific price, and high degree of maturity, a lead-acid BESS is chosen for this study. The performance and cost parameters of the BESS are obtained from [27]. The charging and discharging efficiencies of the BESS are both 95%. The variable installation costs associated with the power and energy capacities are 1,407 $/kW and 275 $/kWh, respectively. The fixed O&M cost is 26.8 $/kW-year, and the variable O&M cost is 0.0011 $/kWh discharged. The BESS power size is considered to be a multiple of 30 kW, and the energy/power ratio varies between 1 and 5.

The estimation of λ is based on the following assumptions:

1) The PEVs operate with an SOC window of 70% (between 20% and 90%).
2) The vehicles are assumed to be fully charged at home before leaving on a trip, and fast charging will complement the home charging.
3) The data collected for NHTS reportedly represents 1,000,000 trips and 300,000 vehicles, but after consideration of four types of vehicles (automobiles, sports vehicles, vans, and pickup trucks) and excluding missing data, 850,000 trips and 150,000 vehicles have been taken into account for this study.
4) The detailed study presented in this paper considers a fully charged PEV20, *i.e.*, a compact sedan, with a battery capacity of 6.51 kWh, which can drive up to 20 miles on electricity. However, a variety of PEV battery types, *i.e.*, PEV40 and PEV60, have been taken into consideration to demonstrate their impact on charging demand and EVCF design. The PEV40 and PEV60 vehicles are compact sedans, with battery capacities of 10.4 kWh and 15.6 kWh, which can drive up to 40 and 60 miles on electricity, respectively [28].

V. Results and Discussions

A. PEV Charging Loads & Impact on EVCF Configuration

To estimate the expected PEV charging demand, the arrival rate of PEVs at an EVCF must first be determined. Fig. 4 shows the probability of PEV20 arrival at an EVCF, determined using the proposed VDT. The arrival rate of PEVs at an EVCF is obtained by multiplying the total estimated number of PEVs to be served at the EVCF, on a typical day, by the PEV arrival probability. Using the arrival rate of PEVs and the QM, the expected PEV charging demand can then be estimated, as illustrated in Fig.5.

In order to maintain the queuing system stability, it is found that four fast chargers are sufficient for a medium PEV penetration level, while five fast chargers are required for high PEV penetration. The power of each fast charger is assumed to be 50 kW, and assuming a 25% margin, the four- and five-port facilities require a 250 kW and a 350 kW transformer on site, respectively. According to the QM, the EVCF is fully occupied from hour 12 to hour 18; the average waiting time in the queue is 1.13 min in year-0 and 20 min at the peak hour in year-10 for medium PEV penetration. For the waiting time to be acceptable in year-10, an additional port must be installed after year-9, but probably there is no necessity for it to be installed prior to year-9 because the average wait is 10 min during that year. The determination of the optimal number of fast chargers, however, is outside the scope of this paper since prior existence of the EVCF is assumed.

In case of high PEV penetration, the average waiting times in the queue are 1.02 min in year-0 and 8.14 min in year-10, which are acceptable. A reasonable conclusion is that a 5-port facility is a suitable choice because it can ensure queuing system stability for high penetration and reduce the waiting time for medium penetration.

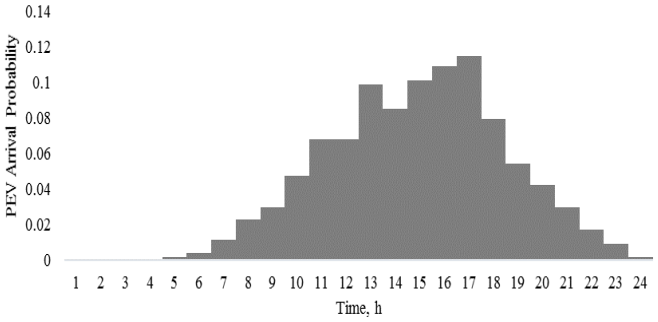

Fig. 4. Probability of PEV20 arrival at an EVCF in the distribution system.

In order to validate the assumption of infinite waiting spaces at the EVCF, two cases are considered: a) an EVCF with *k=10*, *i.e.*, 5 chargers and 5 waiting spaces; and b) an EVCF with *k=20*, *i.e.*, 5 chargers and 15 waiting spaces. These two cases demonstrate the effect of a small and a large limited capacity EVCF, and the impact on number of PEVs rejected from entering the *M/M/c/k* queuing system. The impact of using *M/M/5/10* and *M/M/5/20* queuing models is tested for the period when PEV arrival rate at the EVCF is the highest (worst condition), which is in year-10 of the planning horizon, and hour-17 of the day. The mathematical formulation of an *M/M/c/k* queuing model can be found in [13].

From the results it is noted that with the *M/M/5/10* model, one in forty-four PEV arrivals is rejected, while there is no rejection in the *M/M/5/20* queuing model, and all PEVs enter the EVCF. Thus, the number of PEVs rejected from entering the queuing model is not significant if a finite waiting space is assumed. In view of these results, it is reasonable to assume infinite waiting space at the EVCF, and hence an *M/M/c* queuing model can be used.

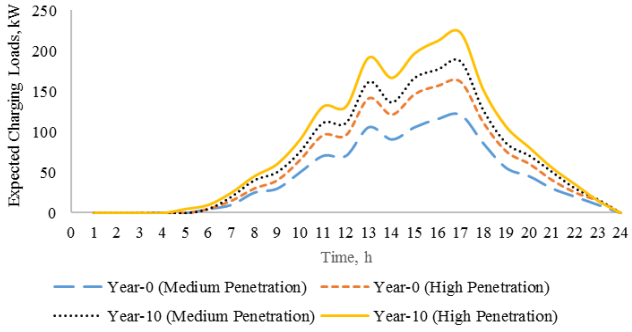

Fig.5. Expected charging demand with PEV20 at an EVCF, for different penetration levels.

B. Investment Decisions and Appropriate Design Options

The load serving capability and the maximum DG penetration at the four chosen EVCF buses, determined using the proposed Distribution Margin Assessment and DG Penetration Assessment models, are shown for year-7 of the planning period in Fig. 6 and 7, respectively. These provide an accurate representation of the limits of the distribution grid at a specific EVCF location.

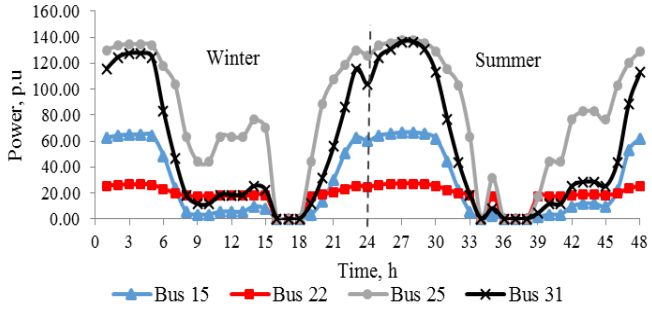

Fig. 6. Load serving capability at EVCF buses in year-7.

The optimal investment decisions for an EVCF at the four chosen locations are determined using the proposed EMA, one of which is provided in Table I. It is realized that at buses 22, 25 and 31, the BESS investment decisions are in the latter part of the planning horizon, which is governed by the load serving capability at these buses and the relatively high cost of BESS as compared to the main grid price. On the other hand, at Bus-15, designing EVCF with BESS (Design-1) is required from year-3 itself since the load serving capability at that bus is lower than the other chosen EVCF locations.

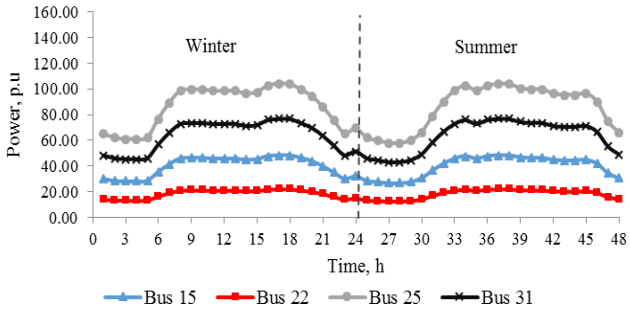

Fig. 7. Maximum DG penetration at EVCF buses in year-7.

It is observed that there is a clear trade-off between the load serving capability and the BESS capacity; the BESS capacity increases as load serving capability decreases. In case of Design-1, the net present value becomes negative at 0.06 $/kWh charging price, and in order to make it profitable for an EVCF and achieve a targeted internal rate of return (IRR) of 14%, PEV charging prices are optimally determined for each location, as shown in Fig. 8. The EVCF located at Bus-25 attains an IRR of 14% with the lowest charging price, while the one at Bus-15 requires the highest charging price.

TABLE I NEW DESIGN DECISIONS OF AN EVCF AT BUS 31

Design Options	Inst. Year	Power Size of BESS (kW)	Energy Size of BESS (kWh)	PV Capacity Size (kW)	IRR%
Design-1: EVCF with BESS	5	150	750		14
	6	30	150		
	7	150	750		
	8	60	300		
	9	60	120		
Design-2: EVCF with Renewable s based DG	1			1000	24
	2			220	
	3			60	
	4			40	
	5			20	
Design-3: EVCF as a Smart Energy Microhub	1	-	-	1000	31
	2	60	300	250	
	3	30	150	40	
	4	-	-	30	
	5	-	-	50	
	6	-	-	20	

The PV generation capacity is governed by the maximum DG capacity that can be accommodated at each site, and hence it varies from one location to another. Consideration of Design-2 results in PEV load shedding or unserved PEVs, as shown in Fig. 9, due to the limited availability of the load serving capability within the planning period as well as the high degree of variability associated with PV generation.

Design-3 is desirable from an investor's perspective, as it results in the highest IRR since a BESS helps to manage the EVCF power consumption, while installing PV generation on a rooftop helps to earn additional revenue.

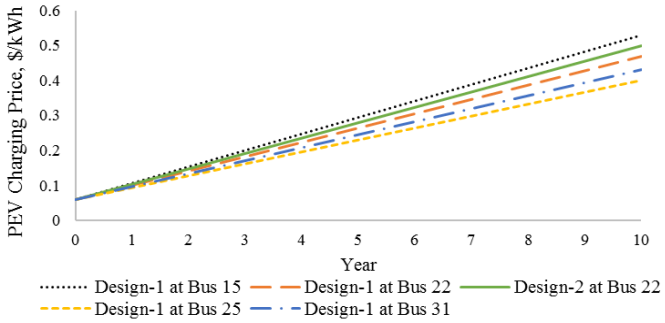

Fig. 8. Optimal PEV20 charging price for 14% targeted IRR at EVCF buses.

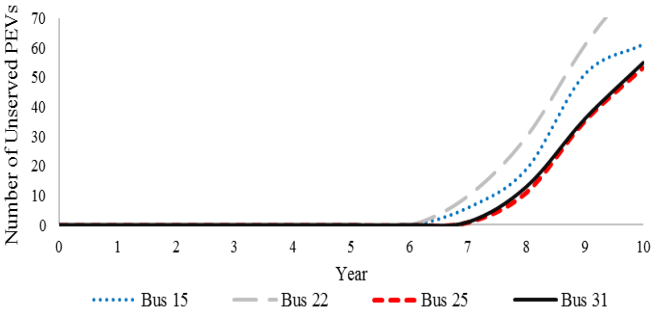

Fig. 9. Number of unserved PEV20 determined from the EAM in Design-2 only, within the planning period.

C. Assessment of Distribution System Capability

To assess distribution system capability in accommodating multiple EVCFs, with and without the new design of EVCF, the Distribution Operation Model is developed. Multiple EVCFs, simultaneously, with and without the proposed EVCF design for the three years (year-0, year-5, year-10) are presented in Table II, considering medium PEV penetration. The base case with no EVCFs, is also presented.

It is worth noting that the unserved energy in year-10 of the base case, can be mitigated by appropriate distribution planning, which is however beyond the scope of this paper. In case of multiple conventional EVCFs, there are several buses where loads are unserved and the LDC has to resort to load curtailment. Thus, there is a need and justification for a new EVCF design that can serve as an energy source and reduce the impact on the distribution system. Year-0 is not considered for EVCFs with the new design as the investment planning starts from year-1. With Desgin-1, a significant reduction in unserved energy is observed, but the LDC still has to resort to load curtailment. There are unserved PEVs in the outcomes of the proposed EAM in case of Design-2, as discussed in the previous section. Therefore, Design-3 achieves the lowest unserved energy, and is valuable from the LDC's perspective, with respect to other EVCF design options.

TABLE II IMPACT OF MULTIPLE EVCFS WITH/WITHOUT NEW DESIGN

Case	Year	Unserved Energy at EVCF Buses (MWh/ 2 days)	Unserved Energy at Other Buses (MWh/ 2 days)
Base case (No EVCFs)	Year-0	-	-
	Year-5	-	-
	Year-10	-	0.120 at Bus 17 2.310 at Bus 18 0.358 at Bus 32 1.132 at Bus 33
Multiple Conventional EVCFs	Year-0	0.037 at Bus 22	-
	Year-5	0.577 at Bus 22	0.736 at Bus 18
	Year-10	1.359 at Bus 15 1.160 at Bus 22	1.188 at Bus 16 1.435 at Bus 17 2.990 at Bus 18 2.621 at Bus 32 1.815 at Bus 33
Multiple EVCFs with Design-1	Year-5	0.546 at Bus 22	0.026 at Bus 18
	Year-10	1.712 at Bus 22	0.036 at Bus 16 0.354 at Bus 17 2.815 at Bus 18 0.242 at Bus 32 1.298 at Bus 33
Multiple EVCFs with Design-2	Year-5	-	-
	Year-10	-	0.369 at Bus 18
Multiple EVCFs with Design-3	Year-5	-	-
	Year-10	-	0.336 at Bus 18

D. Mix of PEV Battery Types and Impact on Probability of PEV Arrival

The studies presented thus far have considered only PEV20 vehicles, but since the electric range of PEV batteries can shape travel patterns, PEV40 and PEV60 vehicles have also been taken into account in order to demonstrate their impact on the probability of PEV arrivals at an EVCF. Fig.10 presents a comparison of the probabilities of PEV arrival at an EVCF for different PEV types. It is noted that, during the early hours of the day, an inverse relationship exists between PEV arrival probability and battery capacity, *i.e.*, PEV arrival probability is higher for PEVs with smaller battery capacities. On the other hand, during the later hours of the day, the relation between PEV arrival probability and battery capacity is proportional, *i.e.*, the PEVs with smaller battery capacity have lower probability of arrival at an EVCF.

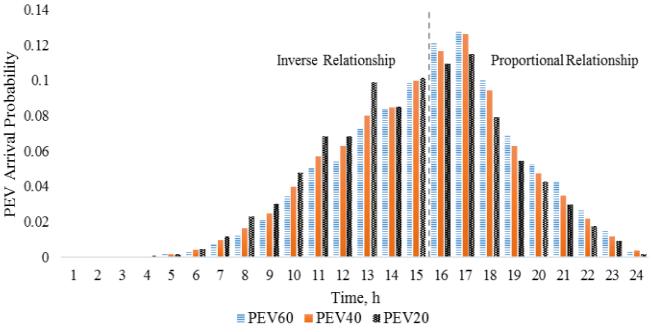

Fig. 10. Probability of PEV arrival at an EVCF.

The charging time of a PEV depends on three factors, its battery capacity, the SOC, and the power level of the charger. Since it is assumed that the PEV operates over an SOC

window of 70% (*i.e.*, between 20% and 90%), the PEV will arrive at the EVCF with SOC = 20%, and leave with 90% SOC. The charging energy required by the PEV is therefore 70% of the battery's energy capacity. The charging time can then be determined by dividing the required charging energy by the power drawn by the fast charger and its efficiency. Hence, the charging durations for PEV20, PEV40, and PEV60 are 6.06, 9.66, and 14.52 min, respectively.

E. Mix of PEV Battery Types and Impact on EVCF Demand

The earlier findings were based on a charging demand for only PEV20 vehicles at an EVCF. This subsection therefore presents the expected EVCF demand associated with a variety of PEV battery capacities, as shown in Fig.11. In the absence of historical data on arrival percentages of PEV types at an EVCF, the PEV arrival rates are assumed based on the different PEV battery capacities. The PEV arrivals is assumed to comprise a mix of 30% PEV20 vehicles, 40% PEV40 vehicles, and 30% PEV60 vehicles; the expected EVCF charging demand is estimated based on these percentages. Understandably, the shape and magnitude of the charging demand profile would differ from the profile with a unique PEV battery type (Fig. 5). Such changes in the magnitude and shape of the EVCF demand profile will have a significant impact on the design of an EVCF as a *smart energy microhub*, and the effect is examined in the following subsection.

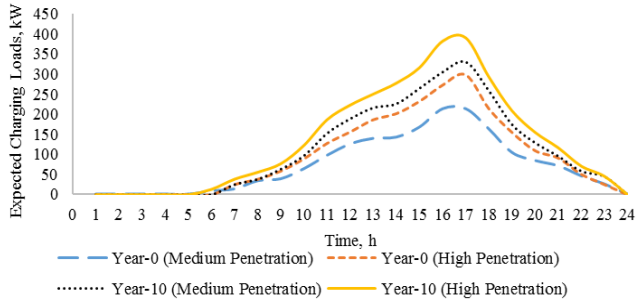

Fig.11. Expected charging demand at an EVCF with a mix of PEV types, for different penetration levels.

F. Charging Demand and Impact on Design of EVCF as a Smart Energy Microhub

When a mix of PEV battery types are considered, and the corresponding demand profile (Fig.11) is taken into account, the design of EVCF as a *smart energy microhub* is expected to be different from the earlier reported design (Table I). Table III presents the new design and it is noted that the power and energy sizing of the BESS increase, and similarly the PV capacity also increases, and the BESS installation years change. Because of the increased capital costs, the IRR of the new EVCF design is 27%, which is lower than the IRR with PEV20 only, which was 31%.

TABLE III DESIGN OF EVCF AS A SMART ENERGY MICROHUB CONSIDERING MIX OF PEV TYPES IMPACTING THE CHARGING DEMAND

Inst. Year	Power Size of BESS (kW)	Energy Size of BESS (kWh)	PV Capacity (kW)	IRR%
1	-	-	1000	27
2	90	450	350	
3	-	-	50	
4	-	-	40	
5	-	-	50	
6	30	150	30	
7	30	150	-	

Since the proposed framework is generic and applicable to any distribution system configuration, the results presented thus far, were not related to a specific geography. However, to demonstrate the relevance of specific geography on the outcomes of the proposed framework, studies are presented in the following subsections considering rural and urban areas.

G. Effect of Specific Geography on PEV Arrival Probability

The data collected by NHTS included both rural and urban areas, but these were not distinguished in the earlier studies presented here. Further data analysis has been carried out to extract the data for rural and urban areas separately, and applied to the VDT, to examine the PEV travel patterns in such areas and their time requirements for fast charging. A comparison of the effects of PEV travel patterns with respect to the probability of PEV arrival at an EVCF in rural and urban areas for PEV20, PEV40, and PEV60 vehicles is presented in Fig.12, Fig.13, and Fig.14, respectively.

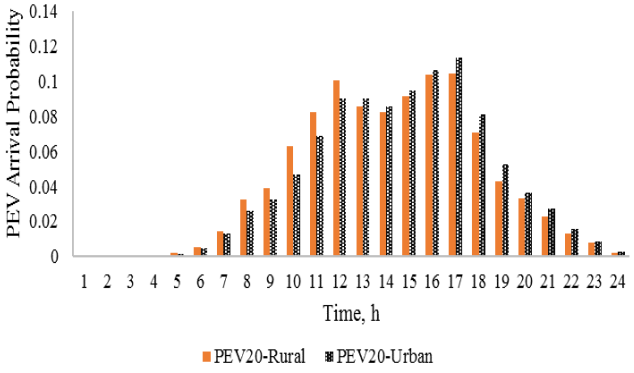

Fig. 12. Probability of PEV20 arrival at an EVCF in rural and urban areas.

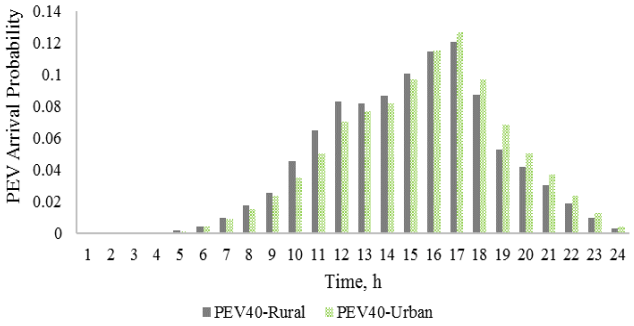

Fig. 13. Probability of PEV40 arrival at an EVCF in rural and urban areas.

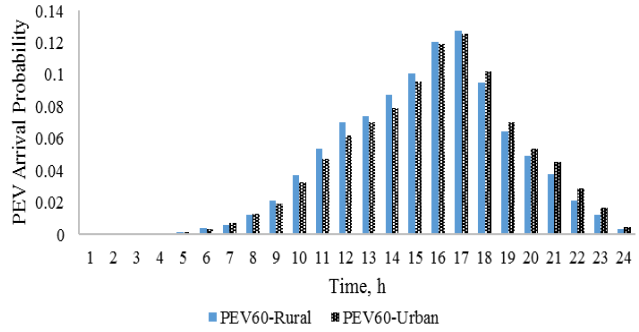

Fig. 14. Probability of PEV60 arrival at an EVCF in rural and urban areas.

It can be seen that PEV charging behavior in rural and urban areas do not differ significantly. However, in rural areas, the probability of PEVs needing fast charging is higher, early in the day. The opposite is true for urban areas, where PEVs are more likely to need fast charging during the night than the day. The results of this comparison are reasonable and valid and are supported by the fact that more real-world activities and movement occur at night in urban than in rural areas

Since the 33-bus system considered in the present study is a radial distribution system of the type more commonly used in rural than in urban areas, the design of an EVCF as a *smart energy microhub* is presented in the following case study for a rural area only. It should be noted that, for an urban area to be considered, the outcomes of the Distribution Margin and DG Penetration Assessment Models, that are indicated in Fig.6 and Fig.7, respectively, for a radial configuration, would change to correspond with a different system configuration. The effects of a rural geography on EVCF demand and design are discussed in the following subsection.

H. Effect of Rural Geography on EVCF Demand

Considering a mix of PEVs, the charging demand at an EVCF in a rural area is estimated, as shown in Fig.15. The rural charging demand profile differs somewhat from the one obtained for the generic case with no specific geography (Fig. 11). The former has only one peak period, *i.e.*, hour 17, while the latter has two peak periods: hours 12 and 17. The following case reveals the significance of such differences with respect to the design of an EVCF as a *smart energy microhub*.

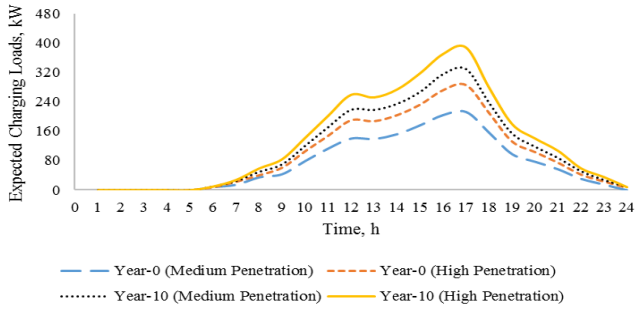

Fig. 15. Expected mixed PEV charging demand at an EVCF in a rural area.

I. Effect of Rural Geography on Design of EVCF as a Smart Energy Microhub

A plan for design of an EVCF as a *smart energy microhub* in a rural area is presented in Table IV. A notable change is evident pertaining to the use of PV capacity rather than BESS, which is installed only at the first year with a high power and energy capacity, while there is an increase in PV capacity, and one more installation year is added.

TABLE IV DESIGN OF EVCF AS SMART ENERGY MICROHUB IN RURAL GEOGRAPHY

Inst. Year	Power Size of BESS (kW)	Energy Size of BESS (kWh)	PV Capacity (kW)	IRR%
1	120	600	1000	27
2	-	-	370	
3	-	-	60	
4	-	-	40	
5	-	-	40	
6	-	-	50	
7	-	-	50	

The cumulative power and energy capacities of the BESS in the rural EVCF are 120 kW and 600 kWh, respectively, in contrast to 150 kW and 750 kWh, respectively, in the generic case in which no geography is specified. On the other hand, the total PV capacity in the rural EVCF is 1,610 kW, while it is 1,520 kW in the generic case. In a rural area, a lower power and energy capacity of BESS is chosen, but more PV units are installed. These findings correlate with the fact that in rural areas, more PEVs need fast charging during the day (Fig.12, Fig.13 and Fig.14), and justifies the increased PV capacity.

Based on the times PEVs need fast charging in rural and urban areas (Fig.12, Fig.13 and Fig.14), and considering the results obtained from the general and rural cases (Table III and Table IV), a reasonable conclusion is that more PV units would be required for EVCF design in a rural area, while more BESS units would be recommended for an urban area EVCF, adjustments that would help match the times PEVs need fast charging during the evening.

With respect to the assessment of distribution system capability, it should be mentioned that, in cases involving mix of PEV types, and/or rural geography, the unserved energy is higher with conventional EVCFs and lower with the new EVCF design, as would certainly be expected. Since the expected charging demand at an EVCF with a mix of PEV types (Fig. 11) is higher than that with PEV20 only (Fig.5), the unserved energy will be higher than that presented in Table II.

VI. CONCLUSIONS

This paper proposed a novel framework for optimal planning and integrating multiple EVCFs in distribution systems. Based on a specific location in the distribution system, and from the perspectives of both the investor and the LDC, the proposed framework determined new design decisions for three investment options for EVCFs commissioned in distribution systems. The effects of different PEV battery types and specific geographies, *i.e.*, rural and urban, on the probability of PEV arrivals at an EVCF were investigated. The proposed EVCF design was examined considering mix of PEV battery types, and a rural geography. The simulation results demonstrate that Design-3 is the most desirable option from the perspectives of both the investor and

the LDC, which transforms the EVCF to a *smart energy microhub*. However, this may not always be true when the distribution system includes DGs. Hence, this research problem becomes more challenging when DGs are considered: What impact does DG allocation have on new EVCF design, and vice versa? These questions will be investigated in future work, as will the distribution system reliability aspect when these design options of EVCFs are presented.

VII. References

[1] D. Sbordone, I. Bertini, B. Di Pietra, M. Falvo, A. Genovese and L. Martirano, "EV fast charging stations and energy storage technologies: A real implementation in the smart micro grid paradigm," *Electr. Power Syst. Res.*, vol. 120, pp. 96-108, 2015.

[2] A. Lam, Y. Leung and X. Chu, "Electric vehicle charging station placement: Formulation, complexity, and solutions," *IEEE Trans. Smart Grid*, vol. 5, pp. 2846-2856, 2014.

[3] M. Geidl, G. Koeppel, P. Favre-Perrod, B. Klockl, G. Andersson, and K. Frohlich,\Energy hubs for the future," *IEEE Power and Energy Magazine*, vol. 5, no. 1, pp. 24{30, Jan.-Feb. 2007.

[4] Z. Liu, F. Wen and G. Ledwich, "Optimal planning of electric-vehicle charging stations in distribution systems," *IEEE Trans. Power Del*., vol. 28, pp. 102-110, 2013.

[5] W. Yao, J. Zhao, F. Wen, Z. Dong, Y. Xue, Y. Xu and K. Meng, "A multi-objective collaborative planning strategy for integrated power distribution and electric vehicle charging systems," *IEEE Trans. Power Syst.*, vol. 29, pp. 1811-1821, 2014.

[6] M. Brenna, A. Dolara, F. Foiadelli, S. Leva and M. Longo, "Urban scale photovoltaic charging stations for electric vehicles," *IEEE Trans. Sustain. Energy*, vol. 5, pp. 1234-1241, 2014.

[7] N. Machiels, N. Leemput, F. Geth, J. Van Roy, J. Buscher and J. Driesen, "Design criteria for electric vehicle fast charge infrastructure based on flemish mobility behavior," *IEEE Trans. Smart Grid*, vol. 5, pp. 320-327, 2014.

[8] U. C. Chukwu and S. M. Mahajan, "V2G parking lot with pv rooftop for capacity enhancement of a distribution system," *IEEE Trans. Sustain. Energy*, vol. 5, pp. 119-127, 2014.

[9] F. Marra, G. Y. Yang, C. Træholt, E. Larsen, J. Ostergaard, B. Blazic and W. Deprez, "EV charging facilities and their application in LV feeders with photovoltaics," *IEEE Trans. Smart Grid*, vol. 4, pp. 1533-1540, 2013.

[10] Y. Liu, Y. Tang, J. Shi, X. Shi, J. Deng and K. Gong, "Application of small-sized SMES in an EV charging station with DC bus and PV system," *IEEE Transactions on Appl. Supercond.*, vol. 25, pp. 1-6, 2015.

[11] National Household Travel Survey [Online]. Available: http://nhts.ornl.gov.

[12] Puget Sound Regional Council (PSRC), "Traffic Choices Study – Summary Report," U.S. Department of Transportation, April 2008.

[13] V. G. Kulkarni, Modeling, Analysis, Design, and Control of Stochastic Systems, 1st ed. New York: Springer, 1999.

[14] G. Li and X.-P. Zhang, "Modeling of plug-in hybrid electric vehicle charging demand in probabilistic power flow calculations," *IEEE Trans. Smart Grid*, vol. 3, no. 1, pp. 492–499, Mar. 2012.

[15] S. Bae and A. Kwasinski, "Spatial and temporal model of electric vehicle charging demand," *IEEE Trans. Smart Grid*, vol. 3, pp. 394-403, 2012.

[16] HydroOne. Technical DG interconnection requirements of HydroOne. [Online]. Available: http://www.hydroone.com.

[17] D. E. Olivares, C. Cañizares and M. Kazerani, "A centralized energy management system for isolated microgrids," *IEEE Trans. Smart Grid*, vol. 5, pp. 1864-1875, 2014.

[18] B. A. Murtagh, M. A. Saunders, and P. E. Gill, GAMS— The Solver Manuals, GAMS Develop. Corp., Washington, DC, USA, 2012. [Online].Available:http://www.gams.com/dd/docs/solvers/ allsolvers.pdf

[19] M. E. Baran and F.F. Wu, "Network reconfiguration in distribution systems for loss reduction and load balancing," *IEEE Trans. Power Del.*, vol.4, pp. 1401-1407, 1989.

[20] J. Pinheiro, C. Dornellas, M. T. Schilling, A. Melo, and J. Mello, "Probing the new IEEE reliability test system (RTS-96): H1-II assessment," *IEEE Trans. Power Syst.*, vol. 13, no.1, pp. 171-176, 1998.

[21] IESO. "Hourly Ontario energy price (HOEP)," Toronto, ON, Canada, [Online]. Available: http://www.ieso.ca.

[22] "Environment assessment of plug-in hybrid electric vehicles," Nationwide Greenhouse Gas Emissions, 1015325, Fin. Rep., EPRI and NRDC, vol. 1, pp. 1–56, 2007.

[23] Y. Zeng, K. C. Land, Z. Wang, and D. Gu, "U.S. Family household momentum and dynamics: An extension and application of the profamy method," Population Res. Policy Rev., vol.25, no.1, pp. 1-41,2006.

[24] J.V. Paatero, P.D. Lund, Effects of large-scale photovoltaic power integration on electricity distribution networks, Renewable Energy 32 (2007) 216–234.

[25] http://www.nrel.gov/docs/fy14osti/62558.pdf

[26] "FIT and microFIT Program," Ontario Power Authority. [Online]. Available: http://fit.powerauthority.on.ca

[27] A. A. Akhil, G. Huff, A. B Currier, B. C. Kaun, D. M. Rastler, S. B. Chen, A. L. Cotter, D. T. Bradshaw and W. D. Gauntlett, "DOE/EPRI 2013 electricity storage handbook in collaboration with NRECA," Report SAND2013-5131, Sandia National Laboratories, 2013.

[28] S. Shafiee, M. Firuzabad, and M. Rastegar, "Investigating the impacts of plug-in hybrid electric vehicles on power distribution systems," *IEEE Trans. Smart Grid*, vol. 4, no. 3, pp. 1351–1360, Sep. 2013.

Walied Alharbi (S'10) received the BSc degree in Electrical Engineering from Qassim University, Saudi Arabia, in 2009, and the MASc degree in Electrical and Computer Engineering from the University of Waterloo, Waterloo, ON, Canada, in 2013, where he is currently working toward the Ph.D. degree. His research interests are in power system flexibility, renewable energy based systems, electric vehicles, and smart grid.

Kankar Bhattacharya (M'95–SM'01) received the Ph.D. degree in electrical engineering from the Indian Institute of Technology, New Delhi, India, in 1993. He was in the faculty of Indira Gandhi Institute of Development Research, Mumbai, India, during 1993–1998, and then the Department of Electric Power Engineering, Chalmers University of Technology, Gothenburg, Sweden, during 1998–2002. He joined the E&CE Department of the University of Waterloo, Waterloo, ON, Canada, in 2003 where he is currently a full Professor. His research interests are in power system economics and operational aspects.